To appear in the *ASCE Journal of Engineering Mechanics*

Phenomenological Model of a Magnetorheological Damper

B.F. Spencer Jr.,[1] S.J. Dyke,[2] M.K. Sain[3] and J.D. Carlson[4]

Abstract

Semi-active control devices have received significant attention in recent years because they offer the adaptability of active control devices without requiring the associated large power sources. Magnetorheological (MR) dampers are semi-active control devices that use MR fluids to produce controllable dampers. They potentially offer highly reliable operation and can be viewed as fail-safe in that they become passive dampers should the control hardware malfunction. To develop control algorithms that take maximum advantage of the unique features of the MR damper, models must be developed that can adequately characterize the damper's intrinsic nonlinear behavior. Following a review of several idealized mechanical models for controllable fluid dampers, a new model is proposed that can effectively portray the behavior of a typical magnetorheological damper. Comparison with experimental results for a prototype damper indicates that the model is accurate over a wide range of operating conditions and is adequate for control design and analysis.

Introduction

Passive and active control systems represent the two ends of the spectrum in the use of supplemental damping strategies for response reduction in civil engineering structures subjected to strong earthquakes and severe winds (see, for example, Soong 1990; Soong, *et al.*, 1991; Housner and Masri 1990, 1993; Housner, *et al.*, 1994). On the other hand, semi-active control systems combine the best features of both approaches, offering the reliability of passive devices, yet maintaining the versatility and adaptability of fully active systems. According to presently accepted definitions, a semi-active control device is one that has properties that can be adjusted in real time but cannot input energy into the system being controlled. Such devices typically have very low power requirements, which is particularly critical during seismic events when the main power source to the structure may fail. Moreover, because many active control systems for civil engineering applications operate primarily to modify structural damping, preliminary studies indicate that semi-active control strategies can potentially achieve the majority of the performance of fully active systems. Various semi-active devices have been proposed which utilize forces generated by surface friction or viscous fluids to dissipate vibratory energy in a structural system. Examples of such devices that have been considered for civil engineering applications include variable orifice dampers (e.g., Shinozuka, *et al*. 1992; Kawashima, *et al.* 1992; Mizuno, *et al.* 1992; Constanti-

1. Professor, Department of Civil Engineering and Geological Sciences, University of Notre Dame, Notre Dame, IN 46556, Member ASCE.
2. Doctoral Candidate and Graduate Research Assistant, Department of Civil Engineering and Geological Sciences, University of Notre Dame, Notre Dame, IN 46556, Student Member ASCE.
3. Freimann Professor, Department of Electrical Engineering, University of Notre Dame, Notre Dame, IN 46556, Member ASCE.
4. Engineering Fellow, Lord Corporation, Mechanical Products Division, Thomas Lord Research Center, 405 Gregson Drive, Cary, NC 27511-7900.

nou, *et al.* 1993; Constantinou and Symans 1994; Sack and Patten 1994; Sack *et al.* 1994; Patten, *et al.* 1994, Kurata, *et al.* 1994), friction controllable braces (*e.g.*, Akbay and Aktan 1990 & 1991; Dowdell and Cherry 1994; Cherry 1994), friction controllable isolators (*e.g.*, Feng and Shinozuka 1990; Kawashima, *et al.* 1992) and variable stiffness devices (Kobori, *et al.* 1993; Inaudi and Kelly 1994).

Another class of semi-active devices uses controllable fluids. The essential characteristic of controllable fluids is their ability to reversibly change from a free-flowing, linear viscous fluid to a semi-solid with a controllable yield strength in milliseconds when exposed to an electric or magnetic field. Two fluids that are viable contenders for development of controllable dampers are: (i) electrorheological (ER) fluids and (ii) magnetorheological (MR) fluids. Although the discovery of both ER and MR fluids dates back to the late 1940's (Winslow 1947; Winslow 1949; Rabinow 1948), research programs have primarily concentrated on ER fluids. A number of researchers have considered electrorheological fluid dampers for civil engineering applications (*e.g.*, Ehrgott and Masri 1992, 1994; Gavin and Hanson 1994; Gavin, *et al.*, 1994; Gavin, 1994; Makris, *et al.*, 1995).

Recently developed MR fluids appear to be an attractive alternative to ER fluids for use in controllable fluid dampers (Carlson 1994; Carlson and Weiss 1994; Carlson, *et al.* 1995; see also: *http://www.rheonetic.com/mrfluid/*). MR fluids are the magnetic analogs of electrorheological fluids and typically consist of micron-sized, magnetically polarizable particles dispersed in a carrier medium such as mineral or silicone oil. When a magnetic field is applied to the fluids, particle chains form, and the fluid becomes a semi-solid and exhibits viscoplastic behavior similar to that of ER fluids. Transition to rheological equilibrium can be achieved in a few milliseconds, allowing construction of devices with high bandwidth. Additionally, Carlson and Weiss (1994) indicated that the achievable yield stress of an MR fluid is an order of magnitude greater than its ER counterpart and that MR fluids can operate at temperatures from –40 to 150^{o}C with only slight variations in the yield stress. Moreover, MR fluids are not sensitive to impurities such as are commonly encountered during manufacturing and usage, and little particle/carrier fluid separation takes place in MR fluids under common flow conditions. Further a wider choice of additives (surfactants, dispersants, friction modifiers, anti-wear agents, *etc.*) can generally be used with MR fluids to enhance stability, seal life, bearing life, *etc.*, since electro-chemistry does not affect the magneto-polarization mechanism. The MR fluid can be readily controlled with a low voltage (*e.g.*, ~12–24V), current-driven power supply outputting only ~1–2 amps. Recognizing the significant potential of devices based on MR fluids, a number of researchers have recently undertaken their study (see, for example, Bossis and Lemaire 1991; Carlson 1994; Carlson and Weiss 1994; Demchuk 1993; Dyke, *et al.* 1996a,b; Fedorov 1992; Grasselli, *et al*. 1993; Horvath and Kopcansky 1993; Kabakov and Pabat 1990; Kashevskii 1990; Kordonsky 1993a,b; Kordonsky, *et al*. 1990, 1993; Lemaire, *et al*. 1994; Minagawa, *et al*. 1994; Pabat 1990; Savost'yanov 1992; and Shulman, *et al*. 1986, 1989; Spencer, *et al.* 1996a,b).

To evaluate the usefulness of MR devices in response reduction for civil engineering structures, a prototype MR damper has been obtained from the Lord Corporation of Cary, North Carolina for laboratory testing. The first step in this evaluation is to develop a high fidelity model for use in control design and analysis. This task is challenging because the MR damper, like most semi-active control means, is a highly nonlinear device. The experimental setup used to obtain the data necessary for identification of a model for the prototype MR damper is discussed in the next section. Then, following a brief review of several idealized models of controllable fluid dampers,

a new phenomenological model is proposed that is numerically tractable and effectively portrays the behavior of an MR damper. Based on the experimental data, a least-squares optimization method is employed to determine appropriate parameters for the analytical model. Comparison with the data indicates that the model presented is accurate for a wide range of operating conditions and is appropriate for use in control algorithm development and system evaluation.

Experimental Setup and Sinusoidal Response Data

To take full advantage of the unique features of the MR damper in control applications, a model must be developed that can accurately reproduce the behavior of the MR damper. The load frame shown in Fig. 1 was designed and built for the purpose of obtaining the MR damper response data necessary for identification studies. In this setup, a double-ended hydraulic actuator, manufactured by Nopak, was employed to drive the damper. The actuator had a 3.8 cm diameter cylinder and a 30.5 cm stroke and was fitted with low-friction Teflon seals to reduce nonlinear effects. A servo-valve, made by Dynamic Valves, Inc., with a nominal operational frequency range of 0–45 Hz was used to control the actuator. A Schaevitz linear variable differential transformer (LVDT) was used to measure the displacement of the piston-rod of the MR damper, and an Omega load cell with a range of ± 4540 N was included in series with the damper to measure the output force. The data acquisition system employed consisted of eight Syminex XFM82 3-decade programmable antialiasing filters having a 90 dB signal to noise ratio and simultaneous sample and hold, an Analogic LSDAS-16-AC-mod2 data acquisition board having 16 bit A/D converters, an Analogic CTRTM-05 counter-timer board, a Gateway 2000 P5-90 computer, and the HEM Data Corporation Snap-Master software. Using this experimental setup, dynamic responses of the damper can be measured for a wide range of prescribed displacement wave forms, including sine, step, triangle and pseudo random.

The prototype MR damper obtained for evaluation is a fixed orifice damper filled with a magnetorheological fluid. The MR fluid is a proprietary formulation, VersaFlo^{TM} MRX-135GD developed by the Lord Corporation, that consists of micron-size, magnetically-soft iron randomly dispersed in a hydrocarbon oil along with additives that promote homogeneity and inhibit gravitational settling. It has a density of 3.28 g/cm^3. The damper is 21.5 cm long in its extended position, and the main cylinder is 3.8 cm in diameter. The main cylinder houses the piston, the magnetic circuit, an accumulator and 50 ml of MR fluid, and the damper has a ± 2.5 cm stroke. As shown in Fig. 2, the MR fluid valve is contained within the damper piston and consists of an annular flow channel having an inner diameter of 27 mm and an outer diameter of 28 mm. The magnetic field is applied radially across the resulting 0.5 mm dimension, perpendicular to the direction of fluid flow. The total axial length of the flow channel is 15 mm of which 7 mm is exposed to the applied magnetic field. Thus, the total volume of fluid that sees the magnetic field at any instant is about

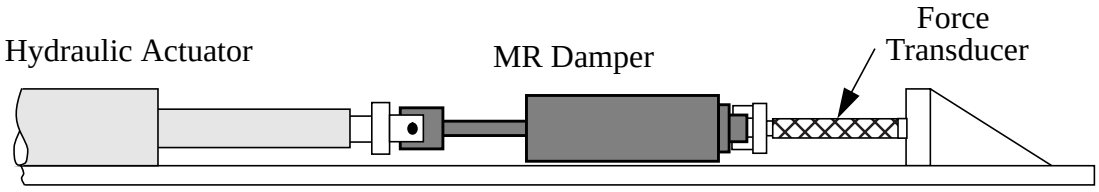

Figure 1. Test Setup for MR Damper Identification.

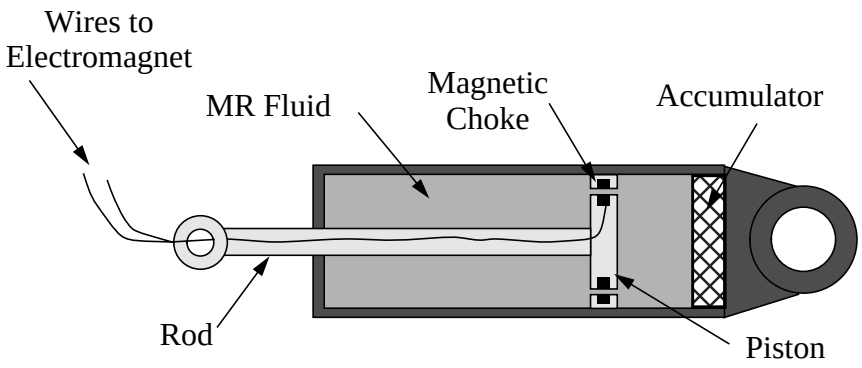

Figure 2. Schematic of MR Damper.

0.3 ml. The magnetic field can be varied from 0 to 200kA/m for currents of 0 to 1 amp in the electromagnet coil, which has a resistance of 4 Ω. The total inductance of the MR fluid valve is 40 mH, resulting in an L/R time constant of 10 msec. The peak power required is less than 10 watts, which would allow the damper to be operated continuously for more than an hour on a small camera battery. For this example, the current for the electromagnet is supplied by a linear current driver running off of 120 volts AC and generates a 0 to 1 amp current that is proportional to a commanded DC input voltage in the range 0–3 V. With this power supply, the damper typically reaches rheological equilibrium in less than 6.5 msec after applying the magnetic field (Carlson and Weiss 1994). Forces of up to 3000 N can be generated with the device, and are stable over a broad temperature range, varying less than 10% in the range of –40 to 150 degrees Celsius.

Using the setup depicted in Fig. 1, a series of preliminary tests was conducted to measure the response of the damper under various loading conditions. In each test, the hydraulic actuator was driven with a sinusoidal signal with a fixed frequency, and the voltage applied to the prototype MR damper was held at a constant level. A wide range of frequencies, amplitudes and voltage levels were considered. The data was sampled at 256 Hz. The velocity response was calculated from the measured displacements via a central difference approximation.

The response of the MR damper due to a 2.5 Hz sinusoid with an amplitude of 1.5 cm is shown in Fig. 3 for four constant voltage levels, 0 V, 0.75 V, 1.5 V, and 2.25 V, being applied to the power amplifier for the device. These voltages correspond to 0 A, 0.25 A, 0.5 A and 0.75 A, respectively. The force generated as a function of time is shown in Fig. 3a, the force-displacement loop is shown in Fig. 3b and the force-velocity loop is shown in Fig. 3c. Note that the force-displacement loops in Fig. 3b progress along a clockwise path with increasing time, whereas the force-velocity loops in Fig. 3c progress along a counter-clockwise path with increasing time.

In Fig. 3, the effects of changing the magnetic field are readily observed. At 0 V the MR damper primarily exhibits the characteristics of a purely viscous device (*i.e.*, the force-displacement relationship is approximately elliptical, and the force-velocity relationship is nearly linear). However, as the voltage increases, the force required to yield the MR fluid in the damper increases and produces behavior associated with a plastic material in parallel with a viscous damper, *i.e.*, Bingham plastic behavior (Shames and Cozzarelli 1992). Also, notice that the increase in force

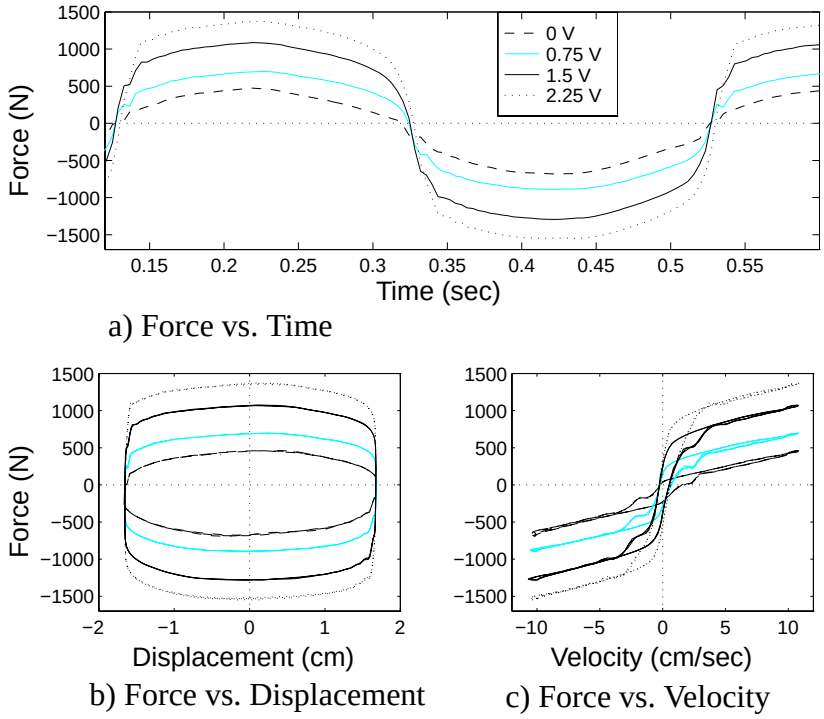

Figure 3. Experimentally Measured Force for 2.5 Hz Sinusoidal Excitation with an Amplitude of 1.5 cm.

for a given increase in the applied voltage is approximately linear for voltages between 0–2.25 V. For the particular damper tested, saturation of the MR effect occurs above 2.25 V.

From Fig. 3, observe that the force produced by the damper is not centered at zero. This effect is due to the presence of an accumulator in the MR damper, which consists of a bladder within the main cylinder (see Fig. 2) that is filled with nitrogen pressurized at 300 psi. The accumulator helps prevent cavitation in the fluid during normal operation and accounts for the volume of fluid displaced by the piston rod as well as thermal expansion of the fluid. From a phenomenological perspective, the accumulator acts like a spring in the damper. In the experimental data provided in Fig. 3, the presence of the accumulator produces an offset in the measured damper force and a slight vertical widening of the response loops in the force-velocity plot. To obtain an effective model of the MR damper, the stiffness associated with the accumulator must be taken into account.

Another interesting feature of the data that is important to note is seen in the force-velocity responses shown in Fig. 3c. Focusing attention on the upper branch of the force-velocity curve, which corresponds to decreasing velocities (*i.e.*, negative accelerations, and therefore positive positions), for large positive velocities, the force in the damper varies linearly with velocity. However, as the velocity decreases and before it becomes negative, the force-velocity relationship is no longer linear, decreasing rapidly and smoothly. This roll-off in the force at small velocities is due to bleed or blow-by of fluid between the piston and the cylinder and is necessary to eliminate harshness from the subjective feel of the damper in vehicular applications. This type of behavior will be sought in a model of the MR damper.

Both nonparametric and parametric models have been considered to model the observed behavior of controllable fluid dampers. Ehrgott and Masri (1994) presented a nonparametric approach for modeling ER fluid dampers by assuming that the damper force could be written in terms of Chebychev polynomials in the damper velocity and acceleration. McClamroch and Gavin (1995) followed a similar approach in modeling an ER device. One of the difficulties in this approach is that the resulting models are often quite complex. Using basic mechanics, Kamath and Wereley (1996) and Makris, *et al.* (1996) have developed parametric models to characterize ER fluids and fluid devices. Alternatively, parametric models based on simple mechanical idealizations have been considered by Stanway, *et al.* (1985, 1987) and Gamota and Filisko (1991) to describe the behavior of controllable fluids and fluid dampers. Such an approach is advocated herein. The next section examines the effectiveness of several idealized mechanical models for predicting the response of the prototype MR damper, and a new model is proposed that addresses a number of shortcomings associated with these models.

Mechanical Model Formulation

The stress-strain behavior of the Bingham viscoplastic model (Shames and Cozzarelli, 1992) is often used to describe the behavior of MR (and ER) fluids. In this model, the plastic viscosity is defined as the slope of the measured shear stress versus shear strain rate data. Thus, for positive values of the shear rate, $\dot{\gamma}$, the total stress is given by

$$\tau = \tau_{y\,(field)} + \eta\dot{\gamma} \tag{1}$$

where $\tau_{y\,(field)}$ is the yield stress induced by the magnetic (or electric) field and η is the viscosity of the fluid.

Based on this model of the rheological behavior of ER fluids, Stanway, *et al.* (1985, 1987) proposed an idealized mechanical model, denoted the Bingham model, for the behavior of an ER damper. The Bingham model consists of a Coulomb friction element placed in parallel with a viscous damper, as shown in Fig. 4. In this model, for nonzero piston velocities, $\dot{x}$, the force generated by the device given by

$$F = f_c \operatorname{sgn}(\dot{x}) + c_0\dot{x} + f_0 \tag{2}$$

where c_0 is the damping coefficient and f_c is the frictional force, which is related to the fluid yield stress. An offset in the force f_0 is included to account for the nonzero mean observed in the

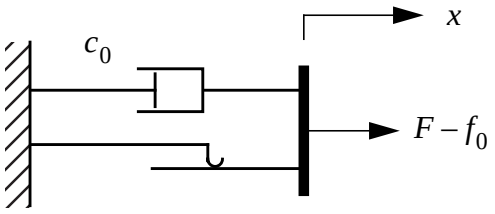

Figure 4. Bingham Model of a Controllable Fluid Damper (Stanway, *et al.* 1985, 1987).

measured force due to the presence of the accumulator. Note that if at any point the velocity of the piston is zero, the force generated in the frictional element is equal to the applied force.

To assess its ability to predict the behavior of the MR damper, the model in (2) was fit to the 2.5 Hz sinusoidal response data shown in Fig. 3 for the case in which the command voltage to the current driver was a constant 1.5 V. The parameters chosen are $f_c = 670$ N, $c_0 = 50$ N $\cdot$ sec/cm and $f_0 = -95$ N. Fig. 5 shows a comparison between the predicted and experimentally obtained responses. Although the force-displacement behavior appears to be reasonably modeled, examination of the force-velocity response and the temporal variation of the force shows that the behavior of the damper is not captured, especially for velocities that are near zero. In particular, this model does not exhibit the nonlinear force-velocity response observed in the data for the case when the acceleration and velocity have opposite signs (or alternatively, when the velocity and the displacement have the same sign) and the magnitude of the velocities are small. While this model may be adequate for response analysis, it is not adequate for control analysis. Notice that the model predicts a one-to-one relationship between the force and velocity, but the experimentally obtained data is not one-to-one. Furthermore, at zero velocity, the measured force has a positive value when the acceleration is negative (positive displacements), and a negative value when the acceleration is positive (negative displacement). This behavior must be captured in a mathematical model to adequately characterize the device for control applications.

Also focusing on predicting the behavior of ER materials, Gamota and Filisko (1991) proposed an extension of the Bingham model, which is given by the viscoelastic-plastic model shown in Fig. 6. The model consists of the Bingham model (*i.e.*, a frictional element in parallel with a dashpot) in series with a standard model of a linear solid (Shames and Cozzarelli, 1992). The governing equations for this model are given by

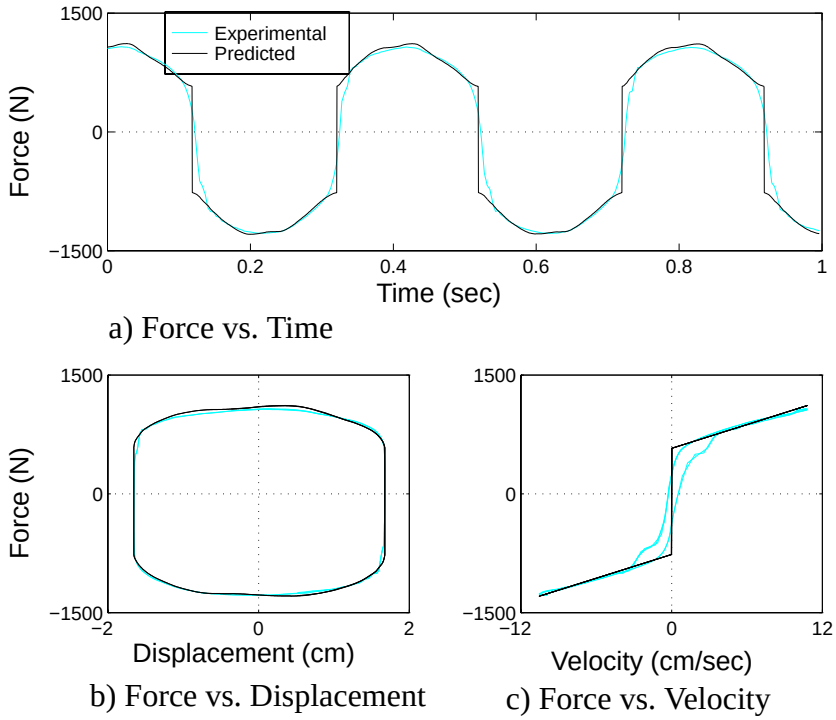

a) Force vs. Time

b) Force vs. Displacement

c) Force vs. Velocity

Figure 5. Comparison Between the Predicted and Experimentally Obtained Responses for the Bingham Model.

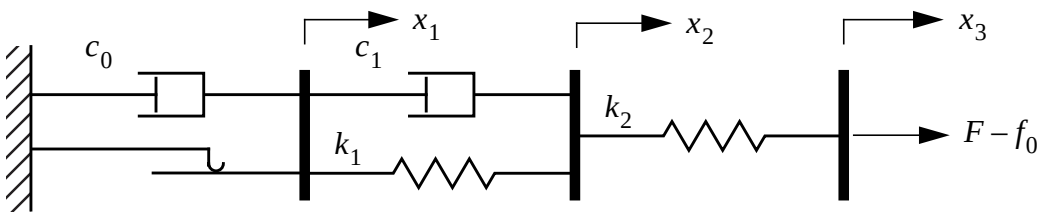

Figure 6. Model proposed by Gamota and Filisko (1991).

$$\left.\begin{aligned} F &= k_1 (x_2 - x_1) + c_1 (\dot{x}_2 - \dot{x}_1) + f_0 \\ &= c_0 \dot{x}_1 + f_c \operatorname{sgn} (\dot{x}_1) + f_0 \\ &= k_2 (x_3 - x_2) + f_0 \end{aligned}\right\} , \qquad |F| > f_c \tag{3}$$

$$\left.\begin{aligned} F &= k_1 (x_2 - x_1) + c_1 \dot{x}_2 + f_0 \\ &= k_2 (x_3 - x_2) + f_0 \end{aligned}\right\} , \qquad |F| \le f_c \tag{4}$$

where c_0 is the damping coefficient associated with the Bingham model and k_1, k_2 and c_1 are associated with the linear solid material. Note that when $|F| \le f_c$, $\dot{x}_1 = 0$.

Again, parameters for the model in (3), (4) were determined to fit the 2.5 Hz data shown in Fig. 3 for the case where the voltage to the current driver was 1.5 V. The parameters chosen are $f_c = 670$ N, $c_0 = 5000$ N $\cdot$ sec/cm, $c_1 = 1300$ N $\cdot$ sec/cm, $k_1 = 5 \times 10^4$ N/cm, $k_2 = 2 \times 10^6$ N/cm and $f_0 = -95$ N. A comparison between the predicted responses and the corresponding experimental data is provided in Fig. 7. As might be expected, this model can portray the force-displacement behavior of the damper well. In addition, it possesses force-velocity behavior that more closely resembles the experimental data. However, the governing equations (3), (4) are extremely stiff, making them difficult to deal with numerically. Numerical integration of (3), (4) for the parameters given previously required a time step on the order of 10^{-6} sec. Note that a decrease in the damping, c_1, can produce the nonlinear roll-off observed in the experimental force-velocity relationship as the velocity approaches zero, but then even smaller time steps are required to simulate the system. The numerical challenges of this model constitute its main shortcoming, which was also noted in Ehrgott and Masri (1994).

One model that is numerically tractable and has been used extensively for modeling hysteretic systems is the Bouc-Wen model (Wen 1976). The Bouc-Wen model is extremely versatile and can exhibit a wide variety of hysteretic behavior. A schematic of this model is shown in Fig. 8. The force in this system is given by

$$F = c_0 \dot{x} + k_0 (x - x_0) + \alpha z \tag{5}$$

where the evolutionary variable z is governed by

$$\dot{z} = -\gamma |\dot{x}| z |z|^{n-1} - \beta \dot{x} |z|^n + A \dot{x} \ . \tag{6}$$

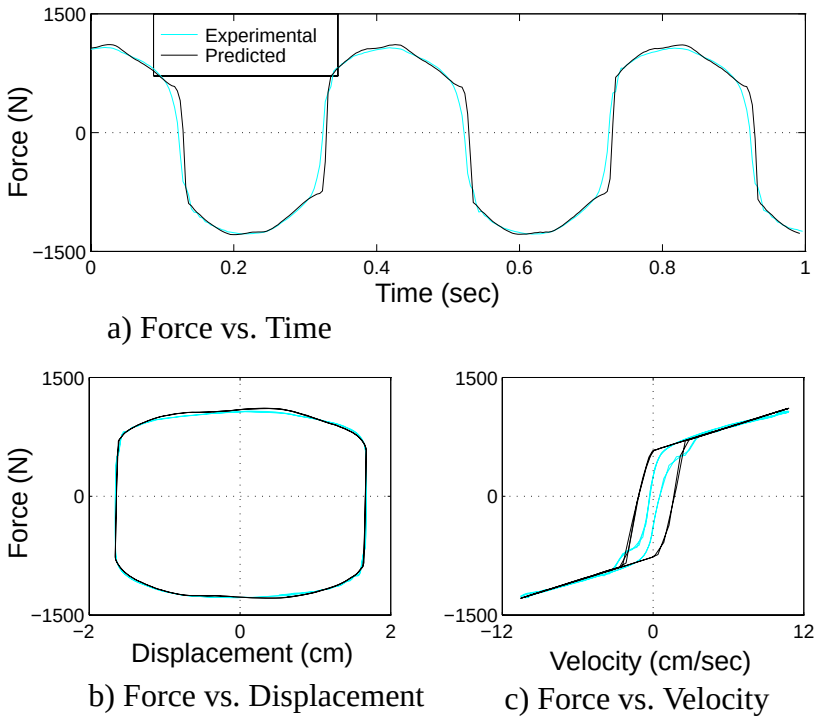

Figure 7. Comparison Between the Predicted and Experimentally Obtained Responses for the Gamota and Filisko Model.

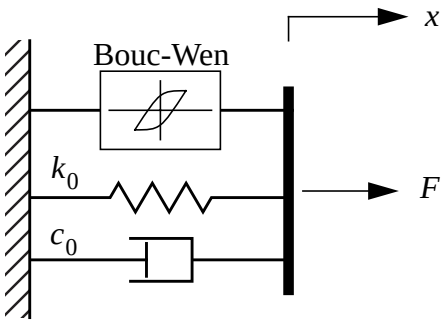

Figure 8. Bouc-Wen Model of the MR Damper.

By adjusting the parameters of the model γ, β and A, one can control the linearity in the unloading and the smoothness of the transition from the pre-yield to the post-yield region. In addition, the force f_0 due to the accumulator can be directly incorporated into this model as an initial deflection x_0 of the linear spring k_0.

A set of parameters was determined to fit the response of the Bouc-Wen model to the experimentally measured response of the MR damper shown in Fig. 3 (2.5 Hz sinusoidal displacement and a constant applied voltage of 1.5V). The parameters for the model in (5), (6) were chosen to be $\alpha = 880$ N/cm, $c_0 = 50$ N$\cdot$sec/cm, $k_0 = 25$ N/cm, $\gamma = 100$ cm^{-2}, $\beta = 100$ cm^{-2}, $n = 2$, $A = 120$ and $x_0 = 3.8$ cm. A comparison between the predicted responses and the cor-

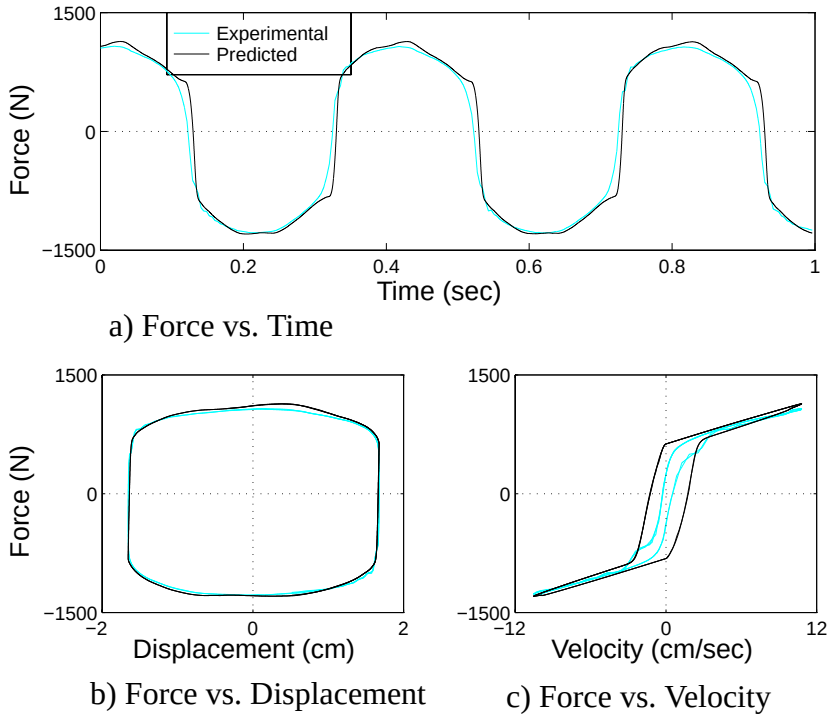

Figure 9. Comparison Between the Predicted and Experimentally Obtained Responses for the Bouc-Wen Model.

responding experimental data is provided in Fig. 9. The Bouc-Wen model predicts the force-displacement behavior of the damper well, and it possesses force-velocity behavior that more closely resembles the experimental data. However, similar to the Bingham model, the nonlinear force-velocity response of the Bouc-Wen model does not roll-off in the region where the acceleration and velocity have opposite signs and the magnitude of the velocities are small. To better predict the damper response in this region, a modified version of the system in Fig. 8 is proposed, as shown in Fig. 10. To obtain the governing equations for this model, consider only the upper section of the model. The forces on either side of the rigid bar are equivalent; therefore,

$$c_1\dot{y} = \alpha z + k_0 (x - y) + c_0 (\dot{x} - \dot{y}) \tag{7}$$

where the evolutionary variable z is governed by

$$\dot{z} = -\gamma|\dot{x} - \dot{y}|z|z|^{n-1} - \beta (\dot{x} - \dot{y}) |z|^n + A (\dot{x} - \dot{y}) \quad . \tag{8}$$

Solving (7) for $\dot{y}$ results in

$$\dot{y} = \frac{1}{(c_0 + c_1)} \{ \alpha z + c_0\dot{x} + k_0 (x - y) \} \quad . \tag{9}$$

The total force generated by the system is then found by summing the forces in the upper and lower sections of the system in Fig. 10, yielding

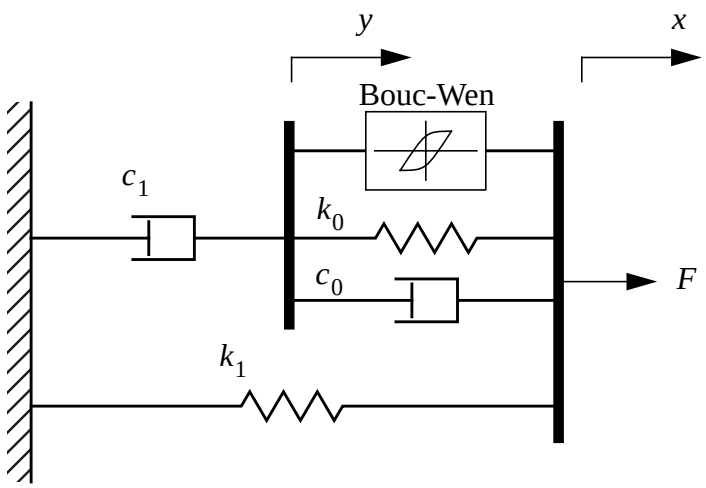

Figure 10. Proposed Mechanical Model of the MR Damper.

$$F = \alpha z + c_0 (\dot{x} - \dot{y}) + k_0 (x - y) + k_1 (x - x_0) \tag{10}$$

From (7), the total force can also be written as

$$F = c_1 \dot{y} + k_1 (x - x_0) \, . \tag{11}$$

In this model, the accumulator stiffness is represented by k_1 and the viscous damping observed at larger velocities is represented by c_0. A dashpot, represented by c_1, is included in the model to produce the roll-off that was observed in the experimental data at low velocities, k_0 is present to control the stiffness at large velocities, and x_0 is the initial displacement of spring k_1 associated with the nominal damper force due to the accumulator.

The parameters for the model in (9), (10) were chosen to be $\alpha = 963$ N/cm, $c_0 = 53$ N $\cdot$ sec/cm, $k_0 = 14$ N/cm, $c_1 = 930$ N $\cdot$ sec/cm, $k_1 = 5.4$ N/cm, $\gamma = 200$ cm^{-2}, $\beta = 200$ cm^{-2}, $n = 2$, $A = 207$, and $x_0 = 18.9$ cm, which fit the response of the proposed model to the 2.5 Hz data shown in Fig. 3 for the case where the voltage to the current driver was 1.5 V. A comparison between the predicted responses and the corresponding experimental data is provided in Fig. 11. The proposed model for the damper predicts the behavior of the damper very well in all regions, including in the region where the acceleration and velocity have opposite signs and the magnitude of the velocities are small.

In addition to the graphical evidence of the superiority of the proposed model, a quantitative study of the errors between each of the models and the experimental data. For each of the models considered here, the error between the predicted force and the measured force has been calculated as a function of time, displacement and velocity over two complete cycles. The following expressions have been used to represent the errors

$$E_t = \frac{\varepsilon_t}{\sigma_F}, \qquad E_x = \frac{\varepsilon_x}{\sigma_F}, \qquad E_{\dot{x}} = \frac{\varepsilon_{\dot{x}}}{\sigma_F} \tag{12}$$

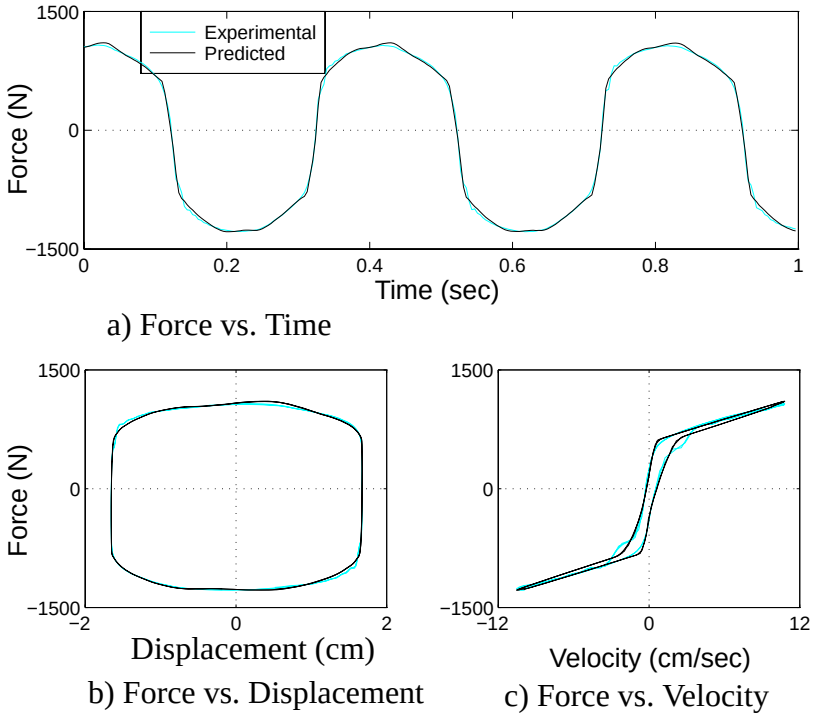

Figure 11. Comparison Between the Predicted and Experimentally Obtained Responses for the Proposed Model.

where

$$\varepsilon_t^2 = \int_0^T (F_{exp} - F_{pre})^2 \, dt \tag{13}$$

$$\varepsilon_x^2 = \int_0^T (F_{exp} - F_{pre})^2 \left|\frac{dx}{dt}\right| dt \tag{14}$$

$$\varepsilon_{\dot{x}}^2 = \int_0^T (F_{exp} - F_{pre})^2 \left|\frac{d\dot{x}}{dt}\right| dt \tag{15}$$

$$\sigma_F^2 = \int_0^T (F_{exp} - \mu_F)^2 \, \mathrm{dt}\,. \tag{16}$$

The resulting normalized errors are given in Table 1. In all cases, the error norms calculated for the proposed model are considerably smaller than those calculated for the other models considered, indicating that the proposed model is superior to the other models for the MR damper considered.

Table 1: Error Norms for MR Damper Models.

Model	E_t	E_x	$E_{\dot{x}}$
Bingham Model	0.154	0.0398	0.133
Gamota and Filisko Model	0.196	0.0717	0.300
Simple Bouc-Wen Model	0.167	0.0585	0.135
Proposed Bouc-Wen Model	0.0351	0.0228	0.0445

Because of its flexibility and numerical tractability for sinusoidal displacement and constant magnetic fields, this model will be the focus of the remainder of the paper. In the next section, a generalization will be considered to model the device when the magnetic field and the prescribed displacements are arbitrary functions of time.

Generalization for Fluctuating Magnetic Fields

All of the data that we have examined previously has been based on the response of the MR damper when the applied voltage, and hence the magnetic field, was held at a constant level. However, optimal performance of a control system which utilizes this device is expected to be achieved when the magnetic field is continuously varied based on the measured response of the system to which it is attached. To use the damper in this way, a model must be developed which is capable of predicting the behavior of the MR damper for a fluctuating magnetic field.

To determine a model that is valid for fluctuating magnetic fields, the functional dependence of the parameters on the applied voltage (or current) must be determined. For instance, the yield stress of the MR fluid is directly dependent on the magnetic field strength, so the parameter α in (9)–(11) is assumed to be a function of the applied voltage. From the experimental results shown in Fig. 3, the steady state yield level appears to vary linearly with the applied voltage, and have a nonzero initial value (*i.e.*, at 0 V). This nonzero initial value is due in part to the fluid which by design has a small yield strength at zero field for stability against gravitational settling, and in part due to friction in the piston rod seal. The viscous damping constants also vary linearly with the applied voltage. Therefore, the following relations are proposed

$$\alpha = \alpha(u) = \alpha_a + \alpha_b u,\ c_1 = c_1(u) = c_{1a} + c_{1b}u \text{ and } c_0 = c_0(u) = c_{0a} + c_{0b}u \qquad (17)$$

where the dynamics involved in the MR fluid reaching rheological equilibrium are accounted for through the first order filter

$$\dot{u} = -\eta(u - v) \qquad (18)$$

and v is the voltage applied to the current driver. Optimal values of a total of fourteen parameters (c_{0a}, c_{0b}, k_0, c_{1a}, c_{1b}, k_1, x_0, α_a, α_b, γ, β, n, η and A) must be determined for the prototype MR damper.

A constrained nonlinear optimization was used to obtain these parameters (Spencer, *et al.* 1996b). The optimization was performed using a sequential quadratic programming algorithm available in MATLAB (1994). Table 2 provides the optimized parameters for the generalized

Table 2: Parameters for the Generalized Model

Parameter	Value	Parameter	Value
c_{0a}	21.0 N·sec/cm	α_a	140 N/cm
c_{0b}	3.50 N·sec/cm·V	α_b	695 N/cm·V
k_0	46.9 N/cm	γ	363 cm^{-2}
c_{1a}	283 N·sec/cm	β	363 cm^{-2}
c_{1b}	2.95 N·sec/cm·V	A	301
k_1	5.00 N/cm	n	2
x_0	14.3 cm	η	190 sec^{-1}

model that were determined to best fit the data in a variety of representative tests, including: 1) step response, 2) constant voltage/random displacement, and 3) random displacement/random voltage. In the following paragraphs these tests will be described, and a comparison made between the data and the responses predicted by the proposed model using the parameters given in Table 2. Simulations were performed in SIMULINK (1994) using the experimentally determined displacement x and calculated velocity $\dot{x}$ of the piston-rod in determining the force generated in the damper model.

The step response tests consisted of applying a triangular displacement to the damper, resulting in regions in which the velocity is nearly constant, and applying a step change in the applied voltage from 0 to 2.25 V as the damper passes through the middle of the stroke ($x \approx 0$). The measured displacement and applied voltage are shown in Fig. 12. The measured force is expected to jump to a new value and remain there when the step in the voltage occurs. Figure 13 compares the predicted results to the experimental data for the input signals shown in Fig. 12. The model effectively predicts the behavior of the device. The error norms given in Eq. (12) were calculated to be $E_t = 0.101$, $E_x = 0.051$, and $E_{\dot{x}} = 0.107$ for this test. This test also verified that the damper reaches rheological equilibrium within approximately 6 msec after the step voltage is applied. Note that the sampling rate was increased to 3 kHz in this test to capture the higher frequency content of the measured responses.

In the second test to verify the model, the damper was excited with a 15 second random displacement record based on an El Centro earthquake acceleration record. A portion of the displacement record of the damper is shown in Fig. 14. The voltage applied to the current driver was a constant 2.25 V. The sampling rate was set at 2 kHz. The simulated force is compared to the experimental data in Fig. 15. As seen here, the model accurately predicts the behavior of the damper. For this test, the error norms given in Eq. (12) were determined to be $E_t = 0.286$, $E_x = 0.118$, and $E_{\dot{x}} = 0.260$.

For the final verification test, the inputs to the device were chosen to be characteristic of the operating conditions the MR damper will experience when it is applied to a structure in a semi-active control system. Dyke, *et al.*, (1996a,b) have proposed a clipped-optimal control strategy for controlling a three story model structure with an MR damper. A controlled simulation was performed based on the numerical example in Dyke, *et al.*, (1996a,b). The input control signal and displacement of the MR damper determined from this simulation are shown in Figure 16. This

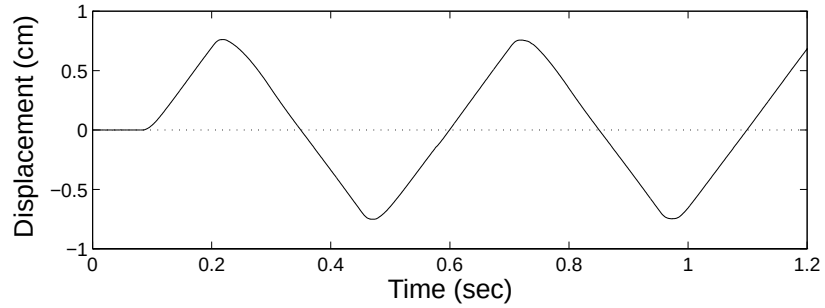

a) Displacement vs. Time

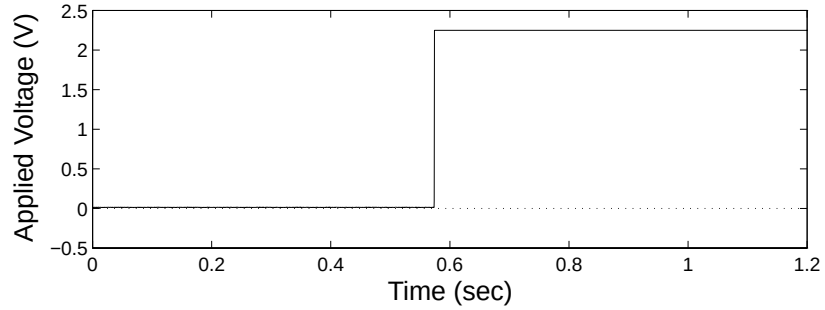

b) Applied Voltage vs. Time

Figure 12. Inputs Applied to the MR Damper in the Step Response Test.

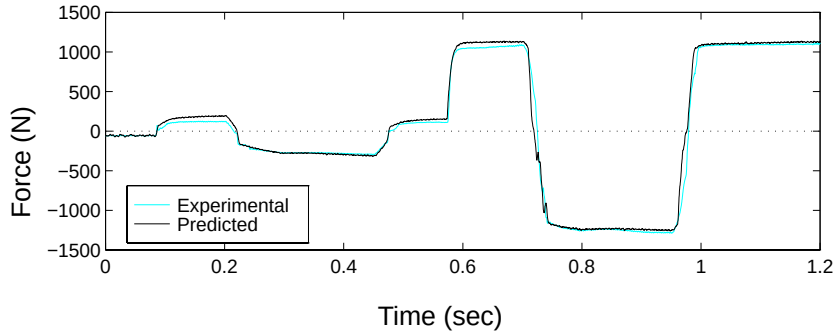

a) Force vs. Time

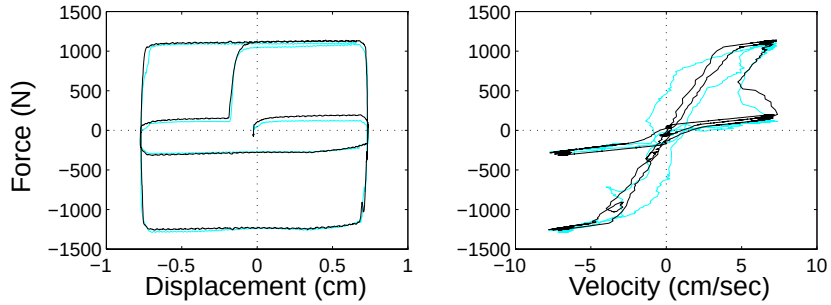

b) Force vs. Displacement c) Force vs. Velocity

Figure 13. Comparison of Predicted Response and Experimental Data for Step Response Tests.

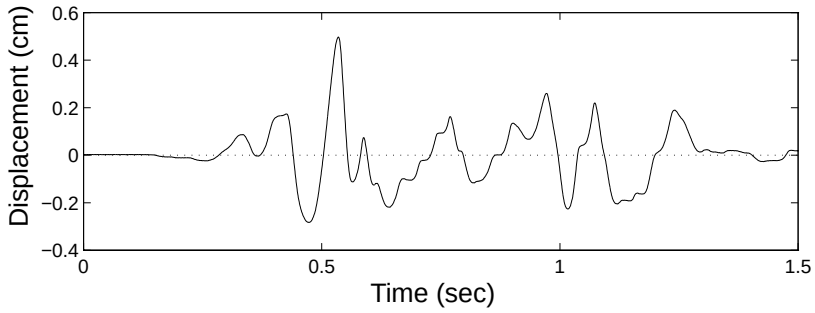

Figure 14. Displacement Input Applied to MR Damper in Constant Voltage, Random Displacement Test.

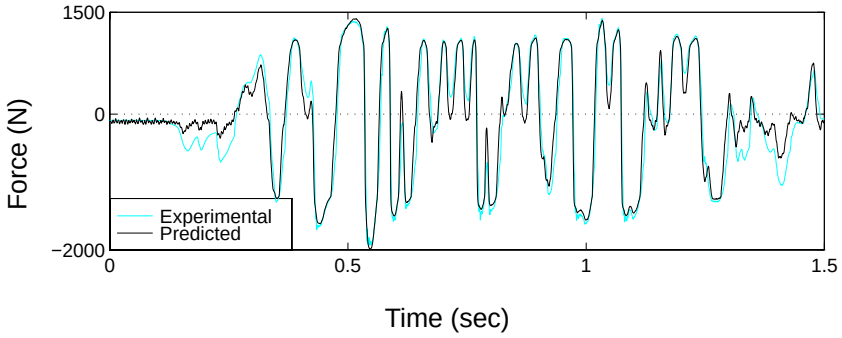

a) Force vs. Time

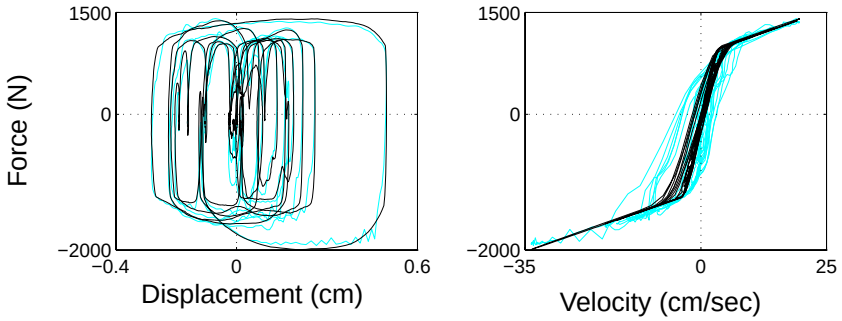

b) Force vs. Displacement

c) Force vs. Velocity

Figure 15. Comparison of the Model Results and the Experimental Data for the Constant Voltage, Random Displacement Tests.

sample displacement and control input history were applied simultaneously to the MR damper. A comparison between the experimental results and the predicted behavior of the damper is shown in Figure 17. Again, excellent agreement is found between the experimental and model responses. For this test, the error norms given in Eq. (12) were determined to be $E_t = 0.188$, $E_x = 0.164$, and $E_{\dot{x}} = 0.188$.

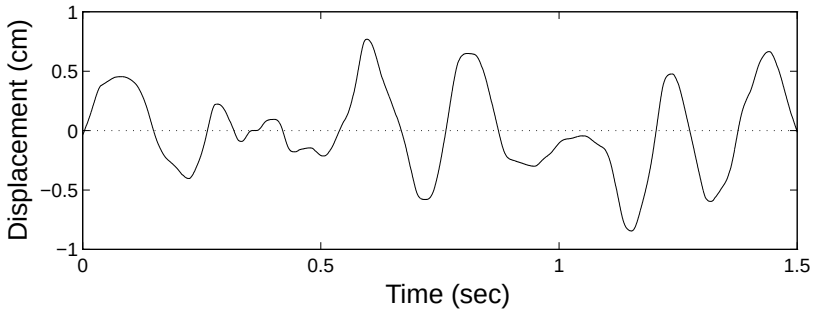

a) Displacement vs. Time

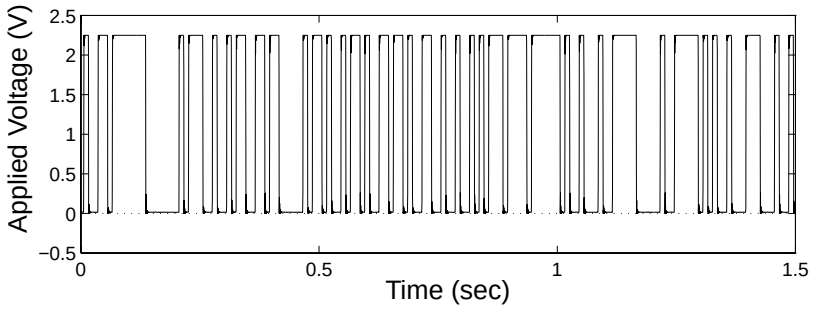

b) Applied Voltage vs. Time

Figure 16. Inputs to MR Damper for the Control Simulation Test.

Conclusion

Recently developed MR fluids have high strength, low viscosity and low power requirements, are stable over a broad temperature range, and are insensitive to impurities commonly introduced during manufacturing. The magnetorheological (MR) damper, consisting of a fixed-orifice damper filled with a controllable MR fluid, is an attractive semi-active control device that appears to have significant potential for structural control applications. To take full advantage of the unique features of the MR damper, a high fidelity model is needed for control design and analysis.

A review of several idealized mechanical models for controllable fluid dampers has been presented. Subsequently, a new model has been proposed that overcomes a number of the shortcomings of these models and can effectively portray the behavior of a typical magnetorheological damper. This phenomenological model is based on a Bouc–Wen hysteresis model, which is numerically tractable and is capable of exhibiting a wide variety of hysteretic behaviors. A dashpot has been added in series with the Bouc–Wen model which creates the nonlinear roll-off observed in the force as the velocity approaches zero; and an additional spring is incorporated into the model to account for the stiffness of the accumulator present in the prototype MR damper. To obtain a model that reproduces the behavior of the damper with fluctuating magnetic fields, three parameters are assumed to vary with the applied voltage. Additionally, a first order filter has been incorporated into the model to account for the dynamics involved in the MR fluid reaching rheological equilibrium. When compared with experimental data, the resulting model was shown to accurate-

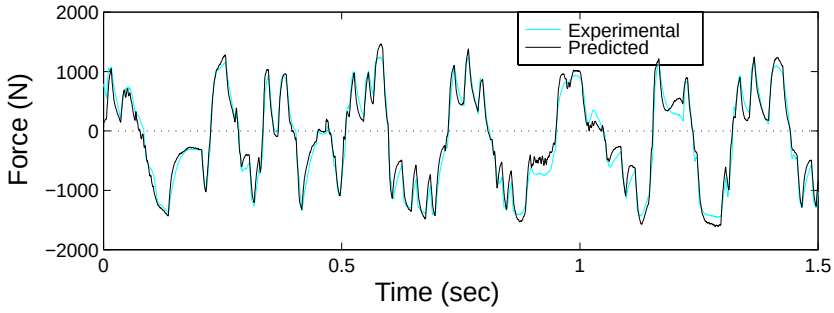

a) Force vs. Time

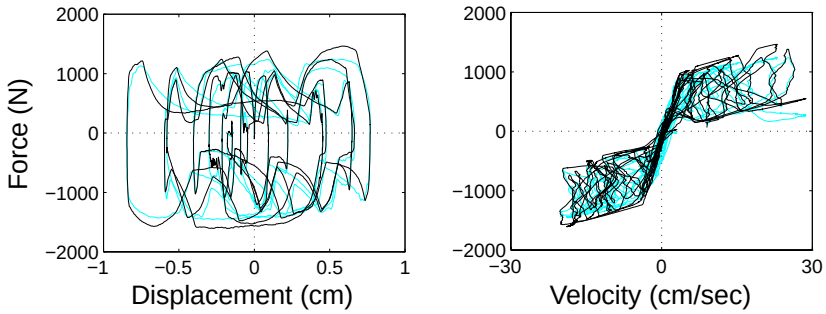

b) Force vs. Displacement c) Force vs. Velocity

Figure 17. Comparison of the Model Results and the Experimental Data for the Control Simulation Test.

ly predict the response of the MR damper over a wide range of operating conditions, including step voltage, random displacement/constant voltage, and random displacement/random voltage tests. These results indicate that the model can be effectively used for control algorithm development and system evaluation.

Acknowledgment

This research is partially supported by National Science Foundation Grant Nos. BCS 93–01584 and BCS95–00301. In addition, the authors from Notre Dame would like to express their appreciation to the Lord Corporation of Cary, North Carolina for providing the prototype magnetorheological damper. In particular, the encouragement and advice of Mr. Thomas Loftus is gratefully acknowledged.

References

Akbay, Z. and Aktan, H.M. (1990). “Intelligent Energy Dissipation Devices.” *Proc. of the Fourth U.S. National Conference on Earthquake Engineering*, Vol 3, No. 4. pp. 427-435.

Akbay, Z. and Aktan, H.M. (1991). “Actively Regulated Friction Slip Devices.” *Proc. of the 6th Canadian Conference on Earthquake Engineering*, pp. 367-374.

Bossis, G. and Lemaire, E. (1991). “Yield Stresses in Magnetic Suspensions,” *Journal of Rheology,* Vol 35(7), pp. 1345–1354.

Carlson, J.D. (1994). “The Promise of Controllable Fluids.” *Proc. of Actuator 94* (H. Borgmann and K. Lenz, Eds.), AXON Technologie Consult GmbH, pp. 266–270.

Carlson, J.D. and Weiss, K.D. (1994). “A Growing Attraction to Magnetic Fluids,” *Machine Design,* August, pp. 61–64.

Carlson, J.D., Catanzarite, D.M. and St. Clair, K.A. (1995). “Commercial Magneto-Rheological Fluid Devices,” *Proceedings of the 5th International Conference on ER Fluids, MR Fluids and Associated Technology,* U. Sheffield, UK.

Carlson, J.D. and Chrzan, M.J., U.S. Patent #5,277,281, “Magnetorheological Fluid Dampers,” 1994.

Carlson, J.D. Chrzan, M.J., and James, F.O., U.S. Patent #5,398,917, “Magnetorheological Fluid Devices,” 1995.

Cherry, S. (1994). “Research on Friction Damping at the University of British Columbia.” *Proceedings of the International Workshop on Structural Control*, USC Publication Number CE-9311, pp. 84-91.

Constantinou, M.C., Symans, M.D., Tsopelas, P. and Taylor, D.P. (1993). “Fluid Viscous Dampers in Application of Seismic Energy Dissipation and Seismic Isolation.” *Proc. of ATC-17-1 Seminar of Seismic Isolation, Passive Energy Dissipation, and Active Control*, Vol. 2, pp. 581-591.

Constantinou, M.C. and Symans, M.D., (1994). “Semi-Active Fluid Viscous Dampers for Seismic Response Control.” *Proc. of the First World Conference on Structural Control*, Pasadena, CA.

Demchuk, S.A. (1993). “Heat Transfer in Narrow Gaps Filled with Magnetorheological Suspensions.” *Journal of Magnetism and Magnetic Materials,* Vol. 122, No. 1 / 3, p. 312.

Dowdell, D.J and Cherry, S. (1994). “Semi-active Friction Dampers for Seismic Response Control of Structures.” Proc. of the Fifth US National Conference on Earthquake Engineering, Vol. 1, pp. 819-828.

Dyke, S.J., B.F. Spencer, Jr., M.K. Sain, and Carlson, J.D. (1996a). “A New Semi-Active Control Device for Seismic Response Reduction,” *Proc. 11th ASCE Engrg. Mech. Spec. Conf.*, Ft. Lauderdale, Florida.

Dyke, S.J., B.F. Spencer, Jr., M.K. Sain, and Carlson, J.D. (1996b). “Seismic Response Reduction Using Magnetorheological Dampers.” *Proc. of the IFAC World Congress*, San Francisco, California.

Ehrgott, R.C. and Masri, S.F. (1992). “Modelling of Oscillatory Dynamic Behavior of Electrorheological Materials in Shear.” *Smart Materials and Structures,* Vol. 4, pp. 275–285.

Ehrgott, R.C. and Masri, S.F. (1994). “Structural Control Applications of an Electrorheological Device.” *Proceedings of the International Workshop on Structural Control*, USC Publication Number CE-9311, pp. 115-129.

Fedorov, V. A. (1992). “Features of Experimental Research into the Characteristics of Magnetorheological and Electrorheological Shock Absorbers on Special Test Stands.” *Magnetohydrodynamics*, Vol. 28, No. 1, p. 96.

Feng, Q. and Shinozuka, M. (1990). “Use of a Variable Damper for Hybrid Control of Bridge Response under Earthquake.” *Proc. of the U.S. National Workshop on Structural Control Research*. USC Publication No. CE-9013, pp. 107–112.

Gamota, D.R. and Filisko, F.E. (1991). “Dynamic Mechanical Studies of Electrorheological Materials: Moderate Frequencies.” *Journal of Rheology*, Vol. 35, pp. 399–425.

Gavin, H.P., Ortiz, D.S. and Hanson, R.D. (1994). “Testing and Modeling of a Prototype ER Damper for Seismic Structural Response Control.” *Proceedings of the International Workshop on Structural Control*, USC Publication Number CE-9311, pp. 166-180.

Gavin, H.P., Hose, Y.D., and Hanson, R.D. (1994). “Design and Control of Electrorheological Dampers.” *Proc. of the First World Conference on Structural Control*, Pasadena, CA, August 3-5, Vol. 1, pp. WP3-83 through WP3-92.

Gavin, H.P. (1994). “Electrorheological Dampers for Structural Vibrations Suppression.” Ph.D. Dissertation, The University of Michigan, Department of Civil and Environmental Engineering.

Kamath, G.M., and Wereley, N.M. (1996). “A Nonlinear Viscoelastic-Plastic Model for Electrorheological Fluids.” *Smart Materials and Structures*, (submitted).

Grasselli, Y., Bossis, G. and Lemaire, E. (1993). “Field-Induced Structure in Magnetorheological Suspensions.” *Progress in Colloid & Polymer Science*, Vol. 93, p. 175.

Horvath, D. and Kopcansky, P. (1993). “Magnetic Dimer Motion Effects in Rotating Magnetic Field (A Qualitative Model of Magnetoviscosity and Permittivity in Magnetorheological Suspensions).” *Czechoslovak Journal of Physics*, Vol. 43, No. 6, p. 671.

Housner, G.W. and Masri, S.F. (Eds.). (1990). *Proceedings of the U.S. National Workshop on Structural Control Research*, USC Publications No. M9013, University of Southern California.

Housner, G.W. and Masri, S.F. (Eds.). (1993) *Proceedings of the International Workshop on Structural Control*, USC Publication No. CE–9311, Univ. of Southern California.

Housner, G.W., Masri, S.F. and Chassiakos, A.G. (Eds.), (1994). *Proceedings of the First World Conference on Structural Control*, Pasadena, CA, August 3-5.

Inaudi, J.A. and Kelly, J.M. (1994) "Experiments on Tuned Mass Dampers Using Viscoelastic, Frictional and Shape-Memory Alloy Materials.” *Proceedings of the First World Conference on Structural Control*, Pasadena, CA, August 3-5, Vol. 2, pp. TP3-107.

Kabakov, A.M. and Pabat, A.I. (1990). “Development and Investigation of Control Systems of Magnetorheological Dampers.” *Soviet Electrical Engineering*, Vol. 61, No. 4, p. 55.

Kashevskii, B.E. (1990). “Relaxation of Viscous Stresses in Magnetorheological Suspensions.” *Magnetohydrodynamics*, Vol. 26, No. 2, p. 140.

Kawashima, K., Unjoh, S. and Shimizu, K. (1992). “Experiments on Dynamics Characteristics of Variable Damper.” *Proc. of the Japan National Symposium on Structural Response Control*, Tokyo, Japan, p.121.

Kobori, T., Takahashi, M., Nasu, T., Niwa, N. and Ogasawara, K. (1993). “Seismic Response Controlled Structure with Active Variable Stiffness System.” *Earthquake Engineering and Structural Dynamics*, Vol. 22, pp. 925–941.

Kordonsky, W.I. (1993a). “Elements and Devices Based on Magnetorheological Effect.” *Journal of Intelligent Material Systems and Structures*, Vol. 4, No. 1, p. 65.

Kordonsky, W.I. (1993b). “Magnetorheological Effect as a Base of New Devices and Technologies.” *Journal of Magnetism and Magnetic Materials*, Vol. 122, No. 1 / 3, p. 395.

Kordonsky, W.I. Shulman, Z.P., Gorodkin, S.R., Demchuk, S.A., Prokhorov, I.V., Zaltsgendler, E.A. and Khusid, B.M. (1990). “Physical Properties of Magnetizable Structure-Reversible Media.” *Journal of Magnetism and Magnetic Materials*, Vol. 85, pp. 114–120.

Kordonsky, W.I., Gorodkin, S.P. and Demchuk, S.A. (1993). “Magnetorheological Control of Heat Transfer.” *International Journal of Heat and Mass Transfer*, Vol. 36, No. 11, pp. 2783.

Kurata, N., Kobori, T., Takahashi, M. Niwa, N. and Kurino, H. (1994). “Shaking Table Experiements of Active Variable Damping System.” *Proceedings of the First World Conference on Structural Control*, Pasadena, CA, August 3-5, pp. TP2-108 through TP2-107.

Lemaire, E., Grasselli, Y. and Bossis, G. (1994). “Field Induced Structure in Magneto and Electro-Rheological Fluids.” *Journal de Physique*, Vol. 2, No. 3, p. 359.

Makris, N., Hill, D., Burton, S. and Jordan, M. (1995). “Electrorheological Fluid Dampers for Seismic Protection of Structures.” *Proc. SPIE Conf. on Smart Struct. and Materials* (I. Chopra, Ed.), San Diego, California, 184–194.

Makris, N., Burton, S.A., Hill, D. and Jordan, M. (1996). “Analysis and Design of an Electrorheological Damper for Seismic Protection of Structures,” *Journal of Engineering Mechanics*, ASCE, (in press).

MATLAB (1994). The Math Works, Inc. Natick, Massachusetts.

McClamroch, N.H. and Gavin, H.P. (1995). “Closed Loop Structural Control Using Electrorheological Dampers.” *Proceedings of the American Control Conference*, Seattle, Washington, pp. 4173–4177.

Minagawa, K., Watanabe, T. and Munakata, M. (1994). “A Novel Apparatus for Rheological Measurements of Electro- Magneto-Rheological Fluids.” *Journal of Non-Newtonian Fluid Mechanics*, Vol. 52, No. 1, p. 59.

Mizuno, T., Kobori, T., Hirai, J., Matsunaga, Y. and Niwa, N. (1992). “Development of Adjustable Hydraulic Dampers for Seismic Response Control of Large Structure.” *ASME PVP Conference*, PVP-Vol. 229, pp. 163–170.

Pabat, A.I. (1990). “Controlled Magnetorheological Shock Absorbers.” *Magnetohydrodynamics*., Vol. 26, No. 2, p. 222.

Patten, W.N., Kuo, C.C., He, Q., Liu, L., and Sack, R.L. (1994). “Suppression of Vehicle-Induced Bridge Vibration via Hydraulic Semiactive Vibrartion Dampers.” *Proc. of the First World Conference on Structural Control*, Pasadena, CA, August 3–5, pp. FA1-30 through FA1-38.

Rabinow, J. (1948). “The Magnetic Fluid Clutch.” *AIEE Transactions*, Vol. 67, pp. 1308–1315.

Sack, R.L. and Patten, W., (1994). “Semiactive Hydraulic Structural Control.” *Proceedings of the International Workshop on Structural Control*, USC Publication Number CE-9311, pp. 417-431.

Sack, R.L., Kuo, C.C., Wu, H.C., Liu, L. and Patten, W.N. (1994). “Seismic Motion Control via Semiactive Hydraulic Actuators.” *Proc. of the U.S. Fifth National Conference on Earthquake Engineering*, Chicago, Illinois, Vol. 2, pp. 311–320.

Savost'yanov, A. (1992). “Effects of Magnetomechanical Relaxation in a Magnetorheological Suspension.” *Magnetohydrodynamics*, Vol. 28, No. 1, p. 42.

Shames, I.H. and Cozzarelli, F.A. (1992). *Elastic and Inelastic Stress Analysis*. Prentice Hall, Englewood Cliffs, New Jersey, pp. 120-122.

Shinozuka, M., Constantinou, M.C. and Ghanem, R. (1992). “Passive and Active Fluid Dampers in Structural applications,” *U.S./China/Japan Workshop on Structural Control*, Shanghai, China, pp. 507–516.

Shulman, Z.P., Kordonsky, W.I. and Zaitsgendler. (1986). “Structure, Physical Properties and Dynamics of Magnetorheological Suspensions.” *International Journal of Multiphase Flow*, Vol. 12, No. 6, pp. 935–955.

Shulman, Z.P., Kordonsky, W.I. and Gorodkin, S.R. (1989). “A Recuperator with a Magnetorheological Coolant.” *Journal of Engineering Physics*, Vol. 56, No. 4, p. 438.

SIMULINK (1994). The Math Works, Inc. Natick, Massachusetts.

Spencer Jr., B.F., Dyke, S.J., Sain, M.K. and Carlson, J.D. (1996a). “Idealized Model of a Magnetorheological Damper,” *Proceedings of the 12th Conference on Analysis and Computation, ASCE*, Chicago, Illinois.

Spencer Jr., B.F., Dyke, S.J., Sain, M.K. and Carlson, J.D. (1996b). “Nonlinear Identification of Semi-Active Control Devices.” *11th ASCE Engrg. Mech. Spec. Conf.*, Ft. Lauderdale, Florida.

Stanway, R. Sproston, J.L. and Stevens, N.G. (1985). “Non-linear Identification of an Electrorheological Vibration Damper.” *IFAC Identification and System Parameter Estimation*, pp. 195–200.

Stanway, R,. Sproston, J.L. and Stevens, N.G. (1987). “Non-linear Modelling of an Electro-rheological Vibration Damper.” *J. Electrostatics*, Vol. 20, pp. 167–184.

Soong, T.T. (1990). *Active Structural Control: Theory and Practice*, Longman Scientific and Technical, Essex, England.

Soong, T.T., Masri, S.F. and Housner, G.W. (1991). “An Overview of Active Structural Control under Seismic Loads.” *Earthquake Spectra*, Vol. 7, No. 3, pp. 483–505.

Wen, Y.K. (1976). “Method of Random Vibration of Hysteretic Systems.” *Journal of Engineering Mechanics Division, ASCE,* Vol. 102, No. EM2, pp. 249–263.

Winslow, W.M. (1947). “Method and Means for Translating Electrical Impulses Into Mechanical Force.” US Patent No. 2,417,850.

Winslow, W.M. (1949). “Induced Fibration of Suspensions.” *Journal of Applied Physics*, Vol. 20, pp. 1137–1140.